JOURNAL OF THE AMERICAN COLLEGE OF CARDIOLOGY VOL. 72, NO. 1, 2018

PUBLISHED BY ELSEVIER

Genome Editing of Induced Pluripotent Stem Cells to Decipher Cardiac Channelopathy Variant

Priyanka Garg, PhD,[a] Angelos Oikonomopoulos, PhD,[a] Haodong Chen, PhD,[a] Yingxin Li, PhD,[a] Chi Keung Lam, PhD,[a] Karim Sallam, MD,[a] Marco Perez, MD,[a,b] Robert L. Lux, PhD,[c] Michael C. Sanguinetti, PhD,[c,d] Joseph C. Wu, MD, PhD[a]

ABSTRACT

BACKGROUND The long QT syndrome (LQTS) is an arrhythmogenic disorder of QT interval prolongation that predisposes patients to life-threatening ventricular arrhythmias such as Torsades de pointes and sudden cardiac death. Clinical genetic testing has emerged as the standard of care to identify genetic variants in patients suspected of having LQTS. However, these results are often confounded by the discovery of variants of uncertain significance (VUS), for which there is insufficient evidence of pathogenicity.

OBJECTIVES The purpose of this study was to demonstrate that genome editing of patient-specific induced pluripotent stem cells (iPSCs) can be a valuable approach to delineate the pathogenicity of VUS in cardiac channelopathy.

METHODS Peripheral blood mononuclear cells were isolated from a carrier with a novel missense variant (T983I) in the KCNH2 (LQT2) gene and an unrelated healthy control subject. iPSCs were generated using an integration-free Sendai virus and differentiated to iPSC-derived cardiomyocytes (CMs).

RESULTS Whole-cell patch clamp recordings revealed significant prolongation of the action potential duration (APD) and reduced rapidly activating delayed rectifier K^+ current (I_{Kr}) density in VUS iPSC-CMs compared with healthy control iPSC-CMs. ICA-105574, a potent I_{Kr} activator, enhanced I_{Kr} magnitude and restored normal action potential duration in VUS iPSC-CMs. Notably, VUS iPSC-CMs exhibited greater propensity to proarrhythmia than healthy control cells in response to high-risk torsadogenic drugs (dofetilide, ibutilide, and azimilide), suggesting a compromised repolarization reserve. Finally, the selective correction of the causal variant in iPSC-CMs using CRISPR/Cas9 gene editing (isogenic control) normalized the aberrant cellular phenotype, whereas the introduction of the homozygous variant in healthy control cells recapitulated hallmark features of the LQTS disorder.

CONCLUSIONS The results suggest that the $KCNH2^{T983I}$ VUS may be classified as potentially pathogenic.
(J Am Coll Cardiol 2018;72:62–75) © 2018 by the American College of Cardiology Foundation.

Congenital long QT syndrome (LQTS) is a potentially lethal genetic disorder of cardiac repolarization that represents a leading cause of sudden cardiac death (SCD) in the young, with a prevalence of ~1 in 2,500 among the general population (1). Among 17 known LQTS subtypes, those associated with mutations in ion channel genes KCNQ1 (LQT1), KCNH2 (LQT2), and SCN5A (LQT3) account for 90% of all genotype-positive cases (2). β-adrenergic blockers are the mainstay of treatment for symptomatic LQTS patients, but implantable cardioverter-defibrillator (ICD), left cardiac sympathetic denervation, and sodium-channel blocker therapy may also be recommended (3,4).

Listen to this manuscript's audio summary by *JACC* Editor-in-Chief Dr. Valentin Fuster.

From the [a]Stanford Cardiovascular Institute and Department of Medicine, Division of Cardiology, Stanford University, Stanford, California; [b]Center for Inherited Cardiovascular Disease, Division of Cardiovascular Medicine, Stanford University, Stanford, California; [c]Nora Eccles Harrison Cardiovascular Research and Training Institute, University of Utah, Salt Lake City, Utah; and the [d]Division of Cardiovascular Medicine, Department of Internal Medicine, University of Utah, Salt Lake City, Utah. Funding support was received from the National Institutes of Health (NIH) through grants T32 EB009035 (to Dr. Garg) and NIH R01 HL113006, NIH R01 HL128170, R01 HL14131, R01 HL130020, and American Heart Association 17MERIT33610009 (to Dr. Wu). All authors have reported that they have no relationships relevant to the contents of this paper to disclose.

Manuscript received December 8, 2017; revised manuscript received March 13, 2018, accepted April 12, 2018.

ISSN 0735-1097/$36.00 https://doi.org/10.1016/j.jacc.2018.04.041

Despite significant advances in the management of LQTS based on an improved understanding of implicated genes and underlying ion currents, the care of almost one-third of LQTS patients remains challenging largely due to low penetrance of clinical symptoms and high variability in phenotypic expression (5). Even multiple family members carrying the same mutation may have different QT intervals and clinical manifestations (6,7). Additionally, the prevalence of asymptomatic individuals with latent LQTS is higher than anticipated (8). This creates a management dilemma of committing patients to lifelong medical therapy that may be risky or unproven, with significant consequences for the patient's quality of life.

SEE PAGE 76

An emerging standard of care for LQTS patients uses clinical genetic testing to identify causal variants in the LQTS susceptibility genes. However, such testing can identify >100 novel nonsynonymous coding variants in any given individual. Ascertaining which, if any, of these is a true causal variant is currently one of the major challenges in the treatment of heritable disorders, especially when the variant is of uncertain significance (VUS) due to inadequate evidence of pathogenicity (9,10). In the era of next-generation sequencing, interpretation of growing numbers of discovered uncertain variants will represent an even greater challenge to therapy (9).

Currently, there are no reliable platforms to predict a priori whether a given variant predisposes an individual to a disease or whether the coding change is benign. The launch of the Precision Medicine Initiative in 2015 has facilitated rapid advances in technologies such as induced pluripotent stem cells (iPSCs) and clustered regularly interspaced short palindromic repeats (CRISPR) genome editing. The creation of isogenic iPSC lines with single-variant changes using CRISPR allows a direct comparison of phenotype at a cellular level. This novel approach of combining these methods can be applied to test the precise phenotypic effect of VUS. Such a strategy may aid in deciphering VUS pathogenicity in LQTS and in tailoring drug treatment and ICD therapy, and could potentially be applied to other inherited cardiac disorders.

By combining patient-specific iPSCs and genome editing, we aimed to develop and validate a human-based platform for elucidating VUS pathogenicity "in a dish" for inherited arrhythmia syndromes and channelopathies. To this end, iPSC lines were derived from a patient carrying the novel variant T983I in the C-terminus of the KCNH2 gene ($KCNH2^{T983I}$), which encodes a channel that mediates the rapidly activating component of the delayed rectifying potassium current (I_{Kr}). Consistent with an LQT2 phenotype, we observed a prolongation of the action potential duration (APD) and reduced I_{Kr} density in VUS-induced pluripotent stem cell-derived cardiomyocytes (iPSC-CMs) compared with cells derived from a healthy control subject. VUS iPSC-CMs were more susceptible to proarrhythmic effects of torsadogenic drugs compared with healthy control iPSC-CMs, whereas treatment of cells with an I_{Kr} activator restored normal APD. Finally, CRISPR/Cas9 genome editing of VUS iPSCs rescued the observed electrophysiological abnormalities, and the introduction of the homozygous variant in a healthy control line recapitulated hallmark LQTS phenotype. Our findings provide important insights into the pathophysiological mechanisms of this previously uncharacterized variant and suggest that the presence of this mutation could be sufficient to induce LQT2.

METHODS

An extended methods section is available in the Online Appendix.

GENERATION OF iPSC LINES. Somatic reprogramming was used to generate iPSC lines from peripheral blood mononuclear cells of the patient with the $KCNH2^{T983I}$ variant as confirmed by RT-PCR and from a healthy subject using the Sendai virus reprogramming protocol, as described previously (11). iPSCs were also derived from an affected patient with a verified LQT2 ($KCNH2^{A561V}$) mutation (12), as described in the previous text. At least 3 colonies were generated from both patients and healthy control subjects. All recruitment and consenting procedures conformed to the Stanford Institutional Review Board–approved protocol.

DIFFERENTIATION OF iPSC-CMs. iPSC-CMs were generated using a 2-dimensional monolayer differentiation protocol and maintained in a 5% CO_2/air environment as previously published (13). Briefly, iPSC colonies were dissociated with 0.5 mmol/l ethylenediaminetetraacetic acid (Gibco, Thermo Fisher Scientific, Waltham, Massachusetts) into single-cell suspension and resuspended in E8 media containing 10 μmol/l Rho-associated protein kinase inhibitor (Sigma-Aldrich, St. Louis, Missouri). Approximately 100,000 cells were replated into Matrigel-coated

ABBREVIATIONS AND ACRONYMS

AP = action potential

APD = action potential duration

Cas9 = CRISPR-associated protein 9

CRISPR = clustered regularly interspaced short palindromic repeats

EAD = early afterdepolarization

hERG = human ether-a-go-go related gene

ICD = implantable cardioverter-defibrillator

I_{Kr} = rapidly activating delayed rectifier K^+ current

iPSC = induced pluripotent stem cell

iPSC-CM = induced pluripotent stem cell–derived cardiomyocyte

LQTS = long QT syndrome

MEA = multielectrode array

SCD = sudden cardiac death

VUS = variant of uncertain significance

VUS^{corr} = genome-edited corrected variant of uncertain significance

VUS^{hom} = genome-edited homozygous variant of uncertain significance

6-well plates. iPSCs were next cultured to 85% cell confluence, and then treated for 2 days with 6 μmol/l CHIR99021 (Selleck Chemicals, Houston, Texas) in RPMI + B27 supplement without insulin to activate WNT signaling and induce mesodermal differentiation. On day 2, cells were incubated in RPMI + B27 without insulin and CHIR99021 (13). On days 3 to 4, cells were treated with 5 μmol/l IWR-1 (Sigma-Aldrich) to inhibit WNT pathway signaling. On days 5 to 6, cells were removed from IWR-1 treatment and placed in RPMI + B27 without insulin. From day 7 onwards, cells were placed in RPMI + B27 with insulin until beating was observed. At this point, cells were glucose-starved for 3 days with RPMI + B27 with insulin to purify iPSC-CMs. Following purification, cells were cultured in RPMI + B27 with insulin. When replating for future use, iPSC-CMs were dissociated with 0.25% trypsin-ethylenediaminetetraacetic acid into a single-cell suspension and seeded on Matrigel-coated plates. Purification by starvation was repeated between days 20 and 23, and differentiated CMs were analyzed on days 30 to 50.

GENOME EDITING. KCNH2 gRNA (5′-CGCCCGGGATACCTGACAGG-3′) was designed using a CRISPR design tool and was subcloned into a plasmid vector (pSpCas9[BB]-2A-GFP) (Addgene, Cambridge, Massachusetts). To introduce the $KCNH2^{2948C>T}$ point mutation into a healthy control iPSC line ($KCNH2^{T983I}$), a single-strand deoxyribonucleic acid oligonucleotide (ssDNA) was designed to contain a single base-pair substitution (C>T) at the respective position. Similarly, a ssDNA containing a single base-pair substitution (T>C) was designed for the correction of the patient $KCNH2^{T983I}$ mutated iPSC line ($KCNH2^{2948C>T}$). Both ssDNAs also contained point mutations of the protospacer adjacent motif sequence to prevent repetitive cutting of genomic DNA by the Cas9 nuclease. The sequence of the ssDNA utilized for gene editing was: 5′ TGCCCTTCTCCAGCCCCAGGCCCCCCGGAGAGCCGCCGGGTGGGGAGCCCCTGATGGAGGACTGCGAGAAGAGCAGCGACATTTGCAATCCTCTGTCAGGTATCCCGGGCGACGGGCGGGCGAGGGA-3′, and the correcting ssDNA oligo was: 5′-TGCCCTTCTCCAGCCCCAGGCCCCCCGGAGAGCCGCCGGGTGGGGAGCCCCTGATGGAGGACTGCGAGAAGAGCAGCGACACTTGCAATCCTCTGTCAGGTATCCCGGGCGACGGGCGGGCGAGGGA-3′.

STATISTICAL ANALYSIS. Statistical significance was determined by unpaired Student's *t*-test (2-tailed), with a single asterisk denoting $p < 0.05$ and considered to be statistically significant; double asterisks indicate $p < 0.01$, and triple asterisks indicate $p < 0.001$ when compared with healthy control iPSC-CMs. The 1-way analysis of variance followed by Tukey's post hoc tests were used when comparing genome-edited iPSC lines.

RESULTS

PATIENT CHARACTERISTICS. The patient is a 39-year-old man with a history of palpitations and pre-syncope. He had multiple electrocardiograms (ECGs) demonstrating QTc intervals from a range of 435 to 485 ms, with 1 very prolonged QTc interval in the recovery phase of exercise testing of 507 ms (**Figures 1A and 1B**). Based on the multiple ECGs demonstrating a prolonged QTc interval in the setting of exertional symptoms and the absence of QT-prolonging medications, the patient was diagnosed with LQTS. The patient's brother had a history of syncope, but ECG revealed a QTc interval of 430 ms. A maternal cousin experienced a cardiac arrest while playing soccer and had an ICD placed, but was not diagnosed with LQTS. The proband patient's maternal grandfather had 4 brothers who all died suddenly under 40 years of age.

Upon genetic testing, the patient was found to have a p.Thr983Ile (c.2948 C>T) variant in the KCNH2 gene (**Figure 1C**) with a population frequency of 0.0001398 in the gnomAD database. Given the population frequency and lack of clear prior phenotypic data, this variant was classified as a variant of uncertain significance. Multiple groups have similarly classified this variant of uncertain significance based on available data (ClinVar for NM_000238.3(KCNH2):c.2948C>T [p.Thr983Ile]). The unrelated healthy subject was an 18-year-old male who had a normal ECG and no personal or family history of syncope or SCD.

GENERATION AND CHARACTERIZATION OF iPSC-CM LINES. iPSCs were derived from the unrelated healthy control subject and the VUS patient harboring the heterozygous c.2948C>T variant in the KCNH2 gene, as described previously (11). Pluripotency of generated iPSC lines was characterized using immunostaining of pluripotency markers such as SOX2 and NANOG (**Figure 1D**). iPSCs were then differentiated into iPSC-CMs as previously described (13) and characterized using immunostaining for cardiac-specific markers, cardiac troponin T and sarcomeric α-actinin (Online Figure 1A). More than 95% of differentiated cells were positively stained for cardiac troponin T (Online Figure 1B).

PATIENT-SPECIFIC VUS iPSC-CMs DISPLAYED AN ABNORMAL ELECTROPHYSIOLOGICAL PROFILE. The action potential (AP) profiles of the healthy control and VUS iPSC-CMs were examined using the standard whole-cell patch clamp technique, and AP parameters such as maximal diastolic potential, overshoot, AP

FIGURE 1 Family Pedigree and Generation of Patient-Specific iPSC Lines

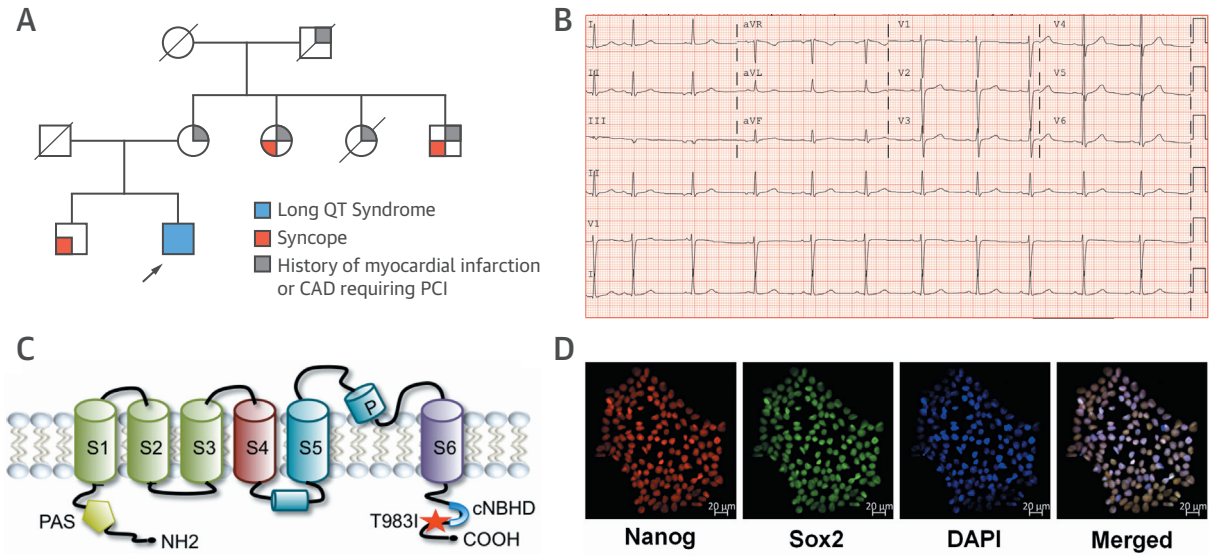

(A) Pedigree of VUS patient. Proband **(arrow)** was diagnosed with LQTS after presenting with prolonged QTc interval (507 ms) on **(B)** surface electrocardiogram. **(C)** Schematic representation of KCNH2 channel protein. **Red star** denotes approximate location of the LQTS variant T983I in the C terminus. **(D)** Representative immunostaining of pluripotency markers SOX2 **(green)** and NANOG **(red)** in iPSC clone derived from the VUS patient. 4′,6-diamidino-2-phenylindole (DAPI) staining **(blue)** indicates the nucleus. CAD = coronary artery disease; cNBHD = cyclic nucleotide binding homology domain; PCI = percutaneous coronary intervention; LQTS = long QT syndrome; VUS = variant of uncertain significance.

amplitude, action potential duration at 50% (APD_{50}) and 90% repolarization (APD_{90}), beating rate, and maximal upstroke velocity (V_{max}) were quantified (Online Table 1). In accordance with the previous published reports (14-16), 3 types of AP morphologies—ventricular-like, atrial-like, and nodal-like—were observed in both healthy control and VUS iPSC-CMs (**Figure 2A**). The AP properties of healthy control iPSC-CMs were similar to those observed in other human iPSC-CM studies (17-19). For most AP parameters, there was no significant difference between healthy control and VUS iPSC-CMs ($p > 0.05$) (Online Table 1). However, both ventricular-like and atrial-like VUS iPSC-CMs displayed significantly prolonged APD_{50} and APD_{90}, respectively (**Figure 2B**). The APD_{90} was 793.7 ± 44.1 ms and 524.1 ± 47.9 ms in VUS iPSC-CMs compared with 367.2 ± 19.6 ms and 288.7 ± 27.7 ms in healthy control iPSC-CMs for ventricular-like and atrial-like cells, respectively. Additionally, mild spontaneous arrhythmogenic activity characterized by beat irregularity or early after depolarizations (EADs) was observed in VUS iPSC-CMs (**Figure 2C**). Whereas 12.9% of VUS iPSC-CMs (n = 130) exhibited EADs, no arrhythmogenic activity was observed in healthy control iPSC-CMs (n = 64).

The in vitro cardiac field potential duration (FPD) on a multielectrode array (MEA) platform has been shown in many studies to correlate with QT interval properties in the ECG (14,15). To evaluate the electrophysiological properties of iPSC-CMs at the multicellular level, we next performed MEA studies and observed that similar to the prolonged APD in patch clamp results, VUS iPSC-CMs had a significantly prolonged field potential duration corrected for variations in beating frequency (FPDc) (522.8 ± 11.4 ms) compared with healthy control subjects (291.2 ± 12.9 ms) (**Figure 2D**) ($p < 0.001$). Collectively, these data indicate that the patient-specific VUS iPSC-CMs display the characteristic hallmarks of the LQTS phenotype.

VUS iPSC-CMs EXHIBITED DECREASED I_{Kr} DENSITY. To investigate the underlying cause of the LQTS phenotype in the patient, ventricular-like iPSC-CMs were subjected to single-cell voltage clamp recordings to measure I_{Kr} density. Using the specific inhibitor E-4031, I_{Kr} was isolated (**Figure 3A**), and its magnitude was found to be markedly reduced in VUS iPSC-CMs compared with that in healthy control iPSC-CMs (**Figures 3B and 3C**). Tail I_{Kr} density was significantly decreased, by 41% to 44%, at voltages from 0 to +40 mV ($p < 0.01$) (**Figure 3C**).

FIGURE 2 Patient-Specific VUS iPSC-CMs Exhibit Characteristic LQTS Signatures

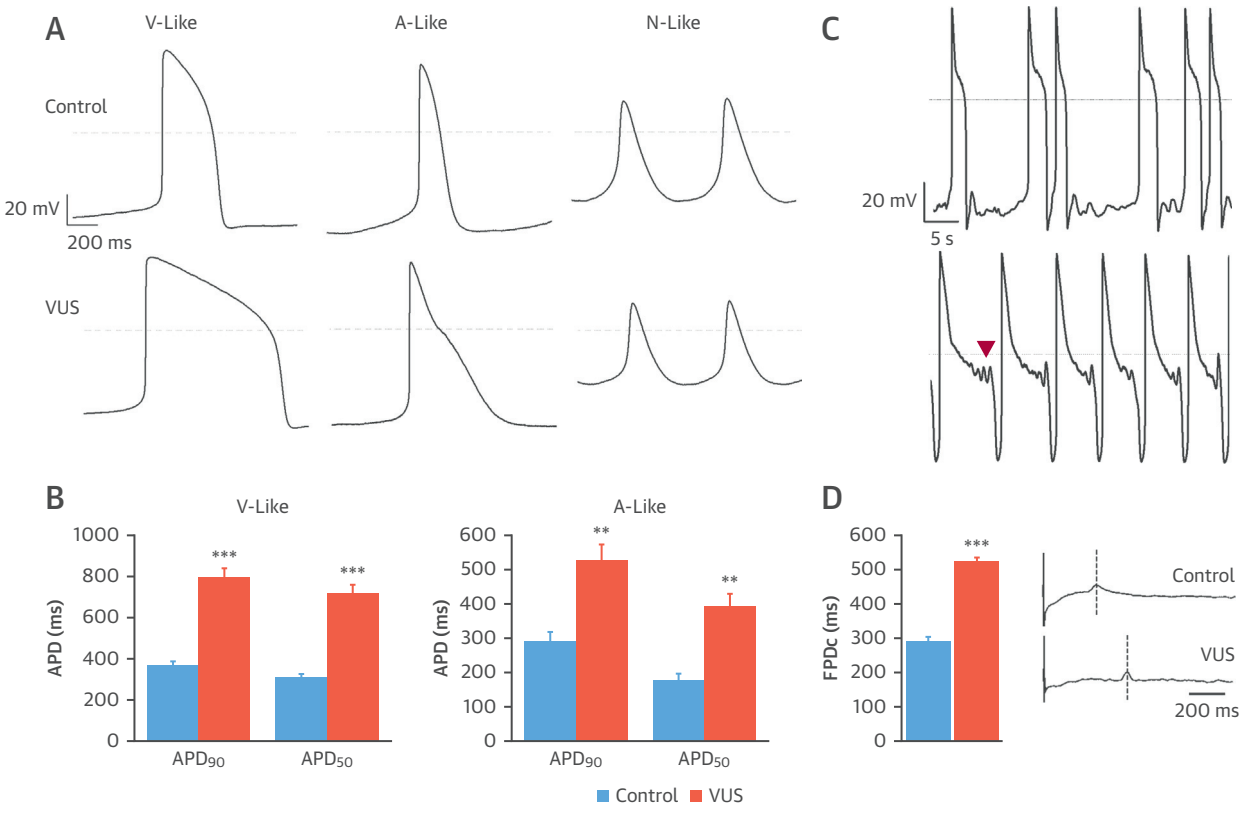

(A) Action potential (AP) recordings from control and VUS iPSC-CMs showing ventricular (V)-like, atrial (A)-like, and nodal (N)-like morphologies. Notice the marked action potential duration (APD) prolongation in both V-like and A-like VUS iPSC-CMs. **(B)** The APD measured at 50% (APD_{50}) and 90% repolarization (APD_{90}) in VUS (**orange**, n = 119) and healthy control (**blue**, n = 49) A-like and V-like iPSC-CMs. ***$p < 0.001$ when compared with control cells. Error bars show SEM. **(C)** Development of spontaneous arrhythmogenicity in VUS iPSC-CMs manifested as beat irregularity **(top)** or early after depolarizations (EADs) indicated by **arrowhead (bottom).** **(D, left)** Summary of rate-matched Fridericia's corrected field potential duration (FPDc) values of VUS iPSC-CMs (**orange**, n = 7) and healthy control (**blue**, n = 7). FPDc = FPD/(beat period)$^{0.3333}$. Error bars show SEM. ***$p < 0.001$. **(D, right)** Representative MEA recordings from healthy control **(top)** and VUS **(bottom)** iPSC-CM monolayer. iPSC-CM = induced pluripotent stem cell-derived cardiomyocyte; other abbreviations as in Figure 1.

In the next set of experiments, we overexpressed the wild type or the variant KCNH2 channel in Xenopus laevis oocytes and recorded I_{Kr} using the 2-electrode voltage-clamp technique. Representative recordings from oocytes injected with either wild-type (human ether-a-go-go related gene [hERG] WT) or VUS KCNH2 (hERG T983I) cRNA are shown in Online Figure 2A. We observed a similar reduction in peak I_{Kr} density (~53%) in 2-electrode voltage-clamp recordings ($p < 0.05$) (Online Figure 2B). These electrophysiological findings were consistent with the channel surface expression in iPSC-CMs. Using Western blot analysis, the differential expression of the mature complex-glycosylated 155 kDa protein band in the VUS iPSC-CMs was found to be significantly reduced compared to healthy control iPSC-CMs, suggesting that mutant channels were not trafficked normally to the cell membrane (Online Figure 3). In addition, the total KCNH2 protein levels were also found to be reduced in VUS iPSC-CMs compared with control iPSC-CMs.

To further determine if the KCNH2 variant could reduce I_{Kr} density in VUS iPSC-CMs by altering channel-gating kinetics, we analyzed voltage dependence of activation parameters (half-maximal voltage [$V_{1/2}$] and slope factor [k]). Interestingly, these parameters were similar between the 2 groups ($V_{1/2}$ = −13.55 ± 2.0 mV for VUS vs. −14.27 ± 2.3 mV for healthy control subjects (**Figure 3D**), suggesting that the variant had no effect on I_{Kr} channel gating. Moreover, biophysical analysis of hERG WT and hERG T983I from Xenopus recordings also confirmed that

FIGURE 3 Single-Cell Voltage-Clamp Recordings Revealed Reduced I_{Kr} Density in VUS iPSC-CMs

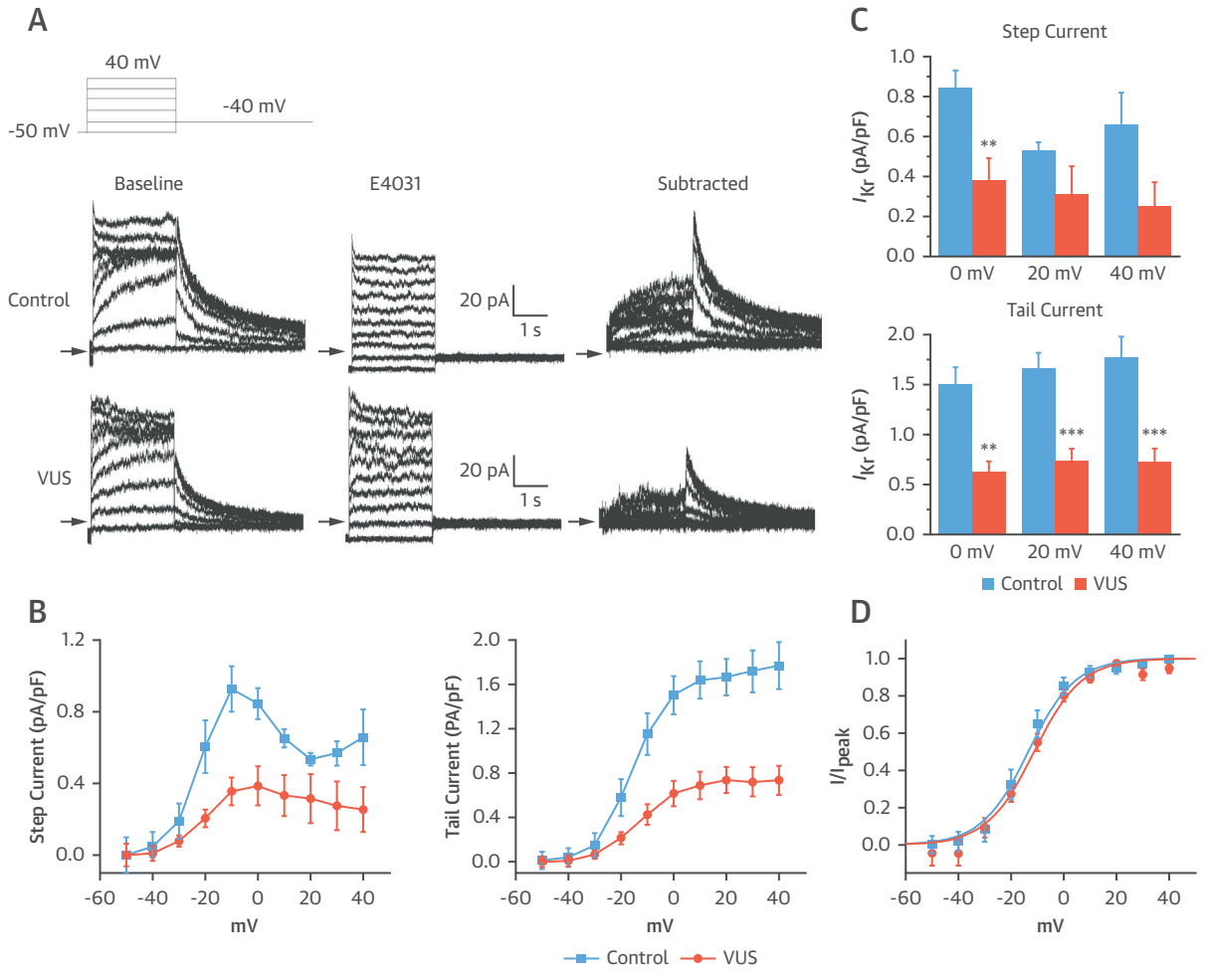

(A) Voltage-clamp recordings of I_{Kr}, measured from healthy control **(top)** and VUS **(bottom)** iPSC-CMs. **(Left)** Baseline recordings. **(Middle)** Recording following administration of E-4031 (2 μmol/l). **(Right)** E-4031-sensitive current (I_{Kr}) defined by digital subtraction of the 2 currents. **Inset:** voltage clamp protocol. **(B)** Average current-voltage (I-V) relationships for I_{Kr} **(left,** step current measured at the end of the test pulses and right, peak tail current) in control **(blue)** and VUS **(orange)** iPSC-CMs. **(C)** Summary of the step current **(top)** and peak tail current **(bottom)** for I_{Kr} density in pA/pF from healthy control **(blue)** ($n = 4$) and VUS iPSC-CMs **(orange)** ($n = 8$) at membrane potentials of 0, +20, and +40 mV (**$p < 0.01$, ***$p < 0.001$). **(D)** Average peak tail current normalized to the maximal current following repolarization to −40 mV (I/I_{peak}) in healthy control **(blue)** and VUS **(orange)** iPSC-CMs. Mean values ± SEM. are shown. $V_{1/2} = -13.55 \pm 2.0$ mV for VUS versus -14.27 ± 2.3 mV for healthy control. Comparison of iPSC lines was performed with 1-way analysis of variance; $p < 0.05$ was considered statistically significant. Abbreviations as in Figures 1 and 2.

the mutant channels exhibited largely similar gating kinetics as the WT channels (Online Figure 2C).

ICA-105574 ENHANCED I_{Kr} AND RESCUED ABNORMAL ELECTROPHYSIOLOGICAL PHENOTYPE IN VUS iPSC-CMs. An interesting approach to treat LQTS is by directly targeting the deficiency in net repolarizing current (20). Recently, Zhang et al. (21) reported that a type II I_{Kr} activator that attenuates channel inactivation shortens APD in iPSC-CMs from LQT1 patients in a dose-dependent manner, whereas a type I compound that slows channel deactivation was ineffective. ICA-105574 (ICA) is a type II I_{Kr} activator that dramatically increases I_{Kr} amplitude in heterologous expression cells, shortens APD in guinea pig ventricular myocytes (22), and shortens QT intervals in isolated guinea-pig hearts as well as in anesthetized dogs (23). However, the effectiveness of ICA in normalizing APD prolongation and suppressing arrhythmia in more physiological human diseased iPSC-CMs has not been previously investigated. Our

FIGURE 4 ICA-105574 Enhanced I_{Kr} Density and Normalized Prolonged APD in VUS iPSC-CMs

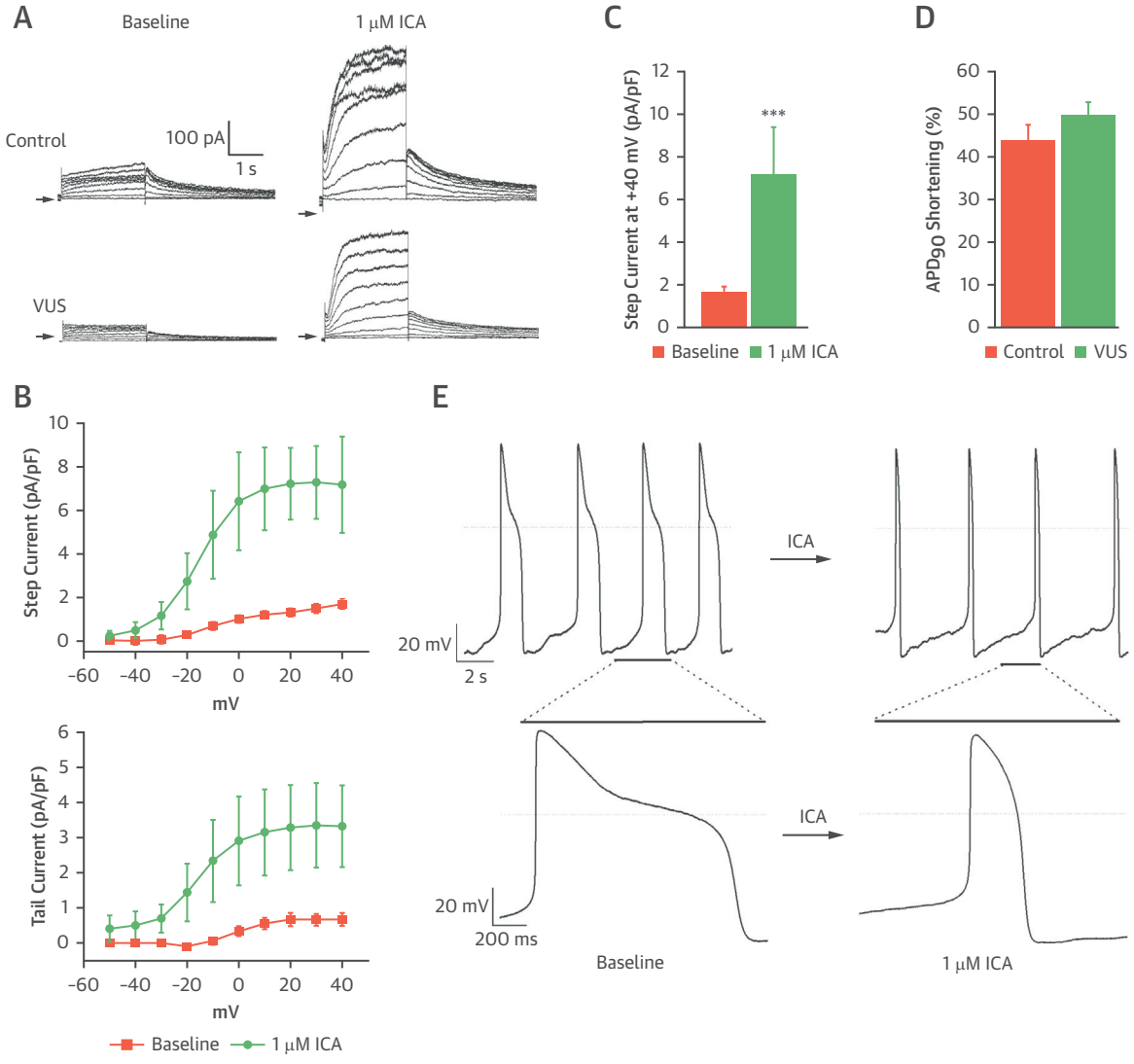

(A) Representative I_{Kr} traces in healthy control **(top)** and VUS **(bottom)** iPSC-CMs at baseline **(left)** and after application of 1 μmol/l ICA-105574, a KCNH2 channel agonist. **(B)** Average I-V curves for I_{Kr} step current **(top)** and peak tail current **(bottom)** density in pA/pF at baseline **(orange)** and after application of 1 μmol/l ICA-105574 **(green)** in VUS iPSC-CMs. **(C)** Summary of average step current density at +40 mV for baseline and 1 μmol/l ICA-105574 in VUS iPSC-CMs ($n = 7$; ***$p < 0.001$). **(D)** Summary of $\%APD_{90}$ shortening induced by ICA-105574 for healthy control and VUS iPSC-CMs ($n = 7$; $p > 0.05$). **(E)** AP recordings at baseline **(left)** and in the presence of 1 μmol/l ICA-105574 **(right)**. Note the severely prolonged APD in VUS iPSC-CMs before application of ICA-105574. An expanded view highlighting a single AP is shown at the **bottom**. Abbreviations as in Figures 1 and 2.

results indicate that ICA is capable of reversing the disease phenotype in VUS iPSC-CMs by drastically increasing the magnitude of I_{Kr} and shortening APD. Notably, the effects of ICA were not limited to VUS iPSC-CMs, but were extended to healthy control iPSC-CMs (Figure 4A). The current voltage relationships of I_{Kr} step currents and tail currents are shown in Figure 4B. ICA (1 μmol/l) increased currents recorded at +40 mV in VUS iPSC-CMs from a basal current density of 1.67 ± 0.23 to 7.16 ± 2.2 pA/pF, a 4.3-fold increase ($p < 0.001$) (Figure 4C). It is important to note here that as ICA is a selective I_{Kr} agonist, we did not use E4031 in these experiments to isolate I_{Kr}.

In the next set of experiments, we evaluated the effect of 1 μmol/l ICA on ventricular APD from healthy control and VUS iPSC-CMs. As anticipated, the

FIGURE 5 Patient-Specific VUS iPSC-CMs and Classical Pathogenic LQT2-A561V iPSC-CMs Displayed Enhanced Susceptibility to Dofetilide-Induced Proarrhythmia

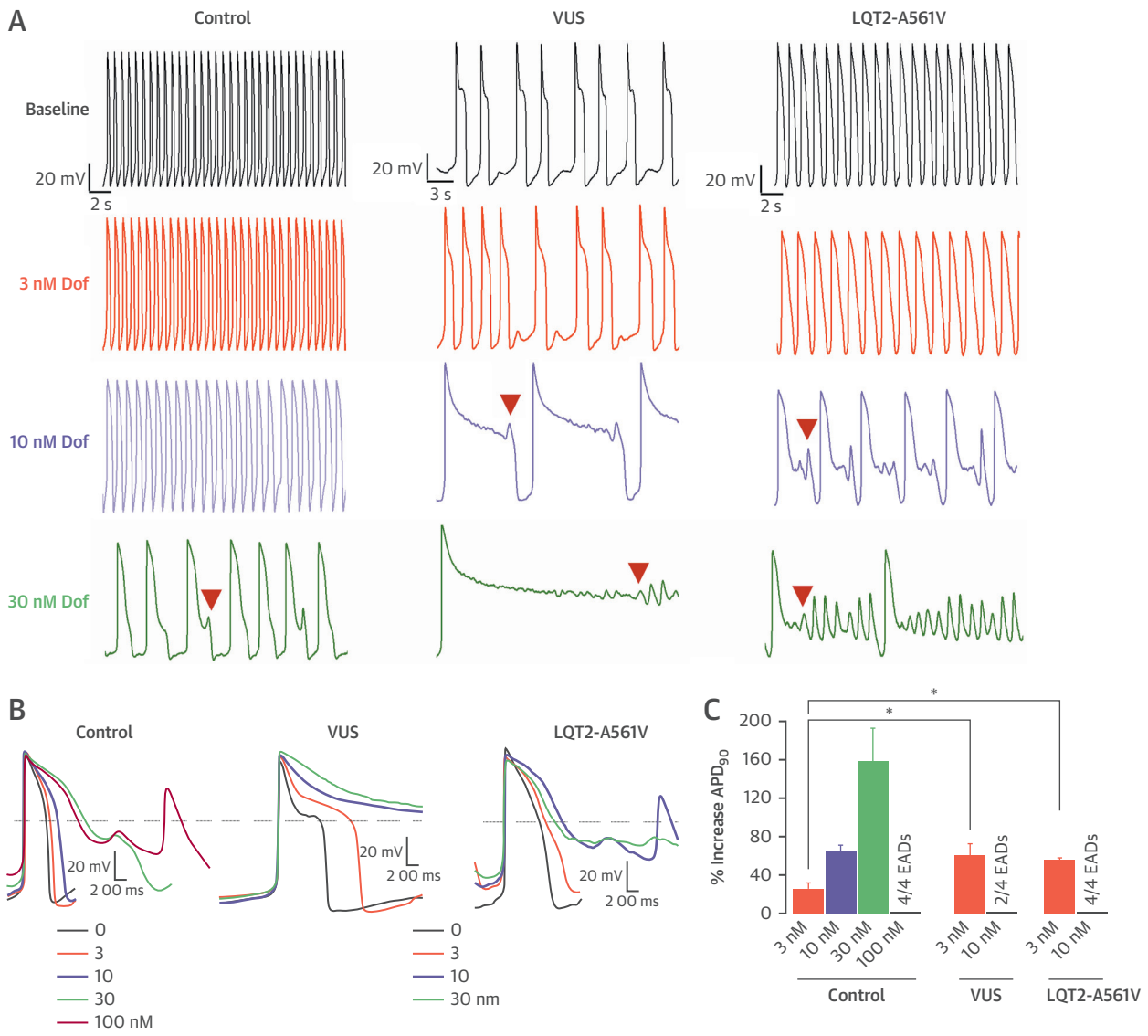

(A) Representative recordings showing dose-dependent effect of dofetilide (Dof) on AP from healthy control **(left)**, VUS **(middle)**, and classical pathogenic LQT2-A561V **(right)** iPSC-CMs (**black** = baseline; **orange** = 3 nmol/l; **blue** = 10 nmol/l; **green** = 30 nmol/l; **red** = 100 nmol/l). **Arrowheads** indicate dofetilide-induced EADs. VUS and LQT2-A561V iPSC-CMs were observed to exhibit dofetilide-induced EADs at lower concentrations (10 nmol/l) as compared with control iPSC-CMs (30 nmol/l). **(B)** Aligned APs showing the effects of dofetilide on control, VUS, and LQT2-A561V iPSC-CMs, respectively (n = 4). **(C)** Percentage increase in steady-state prolongation of APD_{90} by dofetilide at different concentrations for control, VUS, and LQT2-A561V iPSC-CMs. *p < 0.05. Abbreviations as in Figures 1 and 2.

application of ICA produced a rapid shortening of APD in both healthy control and VUS iPSC-CMs, as quantified from the percentage reductions in APD_{90} (Figures 4D and 4E). For 1 μmol/l ICA, APD_{90} was shortened by 43.8 ± 3.8% in healthy control iPSC-CMs (n = 3) and 49.9 ± 3.0% in VUS iPSC-CMs (n = 7, p > 0.05). Our findings suggest that ICA can normalize APD prolongation and prevent cellular arrhythmias in LQTS iPSC-CMs; however, the potential for excessive QT shortening and pro-arrhythmic risks should be carefully considered before further developing type II I_{Kr} agonists.

VUS iPSC-CMs DISPLAYED ENHANCED SUSCEPTIBILITY TO DOFETILIDE-INDUCED PROARRHYTHMIA. We next investigated the proarrhythmic liability of torsadogenic drugs chosen from the CiPA (Comprehensive in Vitro

Proarrhythmia Assay) initiative (24) on healthy control and VUS iPSC lines. We tested 3 high-risk drugs with known QT prolongation effects: dofetilide, ibutilide, and azimilide. These Class III antiarrhythmic drugs selectively block KCNH2 (hERG) channels. Dofetilide induced arrhythmogenicity in both healthy control and VUS iPSC-CMs; however, VUS iPSC-CMs were significantly more susceptible to the proarrhythmic effects of the blocker (**Figures 5A to 5C**). We observed a cut-off concentration (10 nmol/l) at which dofetilide was found to induce EADs in VUS iPSC-CMs, but not in healthy control iPSC-CMs (**Figures 5A and 5B**). We also investigated the effects of dofetilide on KCNH2 channels harboring a verified (classical) LQT2 mutation (LQT2-A561V) (12) by generating iPSC-CMs from an affected patient. iPSC-CMs harboring this mutation were found to have diminished I_{Kr}, prolonged repolarization durations, and elevated baseline arrhythmogenesis (Online Figure 4). Similar to our findings with VUS iPSC-CMs, patient-specific LQT2-A561V iPSC-CMs also displayed arrhythmias starting at 10 nmol/l (**Figures 5A and 5B**), a concentration that was not proarrhythmic for healthy control iPSC-CMs. The enhanced sensitivity of LQT2-A561V and VUS iPSC-CMs to dofetilide-induced toxicity were likely related to drug-induced exacerbation of the baseline arrhythmias in diseased lines as consistent with previous studies (17). Healthy control iPSC-CMs that did not exhibit baseline arrhythmia or APD prolongation required higher doses of dofetilide before exhibiting cardiotoxicity at the single cell level.

Similar to dofetilide, the application of ibutilide (5 nmol/l), a drug used to treat atrial flutter and atrial fibrillation, elicited arrhythmogenicity that manifested as EADs only in VUS iPSC-CMs (Online Figures 5A and 5C). Enhanced arrhythmogenicity with azimilide (1 μmol/l), a drug that is currently in clinical trials, also manifested as EADs only in VUS iPSC-CMs (Online Figures 5B and 5C). Taken together, these findings indicate that VUS iPSC-CMs, which were characterized by an elevated baseline of arrhythmia, exhibited a particular propensity for drug-induced EADs by I_{Kr} blockade. This high frequency of baseline arrhythmias and electrophysiological abnormalities observed in LQT2-A561V and VUS iPSC-CMs may be explained by imbalances in ion channel homeostasis caused by mutations in the KCNH2 gene.

GENOME-EDITED HOMOZYGOUS iPSC-CMs DISPLAYED EXACERBATED LQTS PHENOTYPE. To confirm the role of the $KCNH2^{T983I}$ variant in the generation of an LQTS phenotype, and to assess whether introducing a homozygous variant results in further exacerbation of the arrhythmic phenotype compared with the heterozygous patient iPSC-CMs, we next introduced the homozygous variant in healthy control cells using the CRISPR/Cas9 genome-editing technology (Online Figures 6 and 7). Whole-cell current clamp recordings were performed from single beating iPSC-CMs to obtain spontaneous APs (**Figure 6A**). The key AP parameters were collected and assessed (Online Table 1). The ventricular-like and atrial-like iPSC-CMs derived from genome edited homozygous line (VUS^{hom}) exhibited significantly longer APD_{90} compared with the healthy control line (605.3 ± 72.2 ms vs. 288.7 ± 27.7 ms for atrial-like and 1,207.9 ± 198.3 ms vs. 367.2 ± 19.6 ms for ventricular-like cells, respectively; $p < 0.01$) (**Figure 6B**). Importantly, as anticipated the VUS^{hom} iPSC-CMs displayed a severe arrhythmogenic phenotype (**Figure 6C**) more akin to that observed in the verified LQT2-A561V iPSC-CMs such as the development of EADs or triggered beat (45.2% in VUS^{hom} vs. 12.9% in VUS vs. 46% in LQT2-A561V iPSC-CMs). In conclusion, consistent with our hypothesis regarding the role of this novel variant as an underlying cause of LQTS, VUS^{hom} iPSC-CMs faithfully recapitulated a more severe arrhythmic disease phenotype.

GENOME-EDITED CORRECTED iPSC-CMs ELICITED PHENOTYPIC RESCUE OF REPOLARIZATION ABNORMALITY. We next utilized CRISPR/Cas9-mediated genome editing to correct the $KCNH2^{T983I}$ variant implicated in the presented VUS to validate the pathogenicity of the suspected causative variant (Online Figures 6 and 7). The resultant genome-edited corrected variant of uncertain significance (VUS^{corr}) iPSC-CMs had a correction of the causative KCNH2 variant (rs397514446) and served as an isogenic control line. As shown in **Figure 7**, the VUS^{corr} iPSC-CMs displayed a marked reduction in APD prolongation compared with the VUS iPSC-CMs, without any incidence of EADs or triggered activity, such that the AP recordings resembled those from healthy control lines (APD_{90} of 452.62 ± 3.7 ms and 332.2 ± 61.1 ms in VUS^{corr} vs. 367.17 ± 19.6 ms and 288.73 ± 27.7 ms in healthy control lines for ventricular-like and atrial-like cells, respectively) (**Figures 7A and 7B**). Similar findings were obtained in extracellular MEA recordings (FPDc of 297.4 ± 4.0 ms vs. 291.2 ± 12.9 ms) that revealed a reversal of the LQTS phenotype (**Figure 7C**). Moreover, voltage clamp recordings of I_{Kr} from VUS^{corr} demonstrated a significant increase in tail current density compared to the VUS line (1.46 ± 0.24 pA/pF vs. 0.73 ± 0.13 pA/pF; $p < 0.01$) (**Figures 7D to 7F**). Furthermore, no change was

FIGURE 6 Genome-Edited Homozygous iPSC-CMs Displayed Potentiated LQTS Phenotype

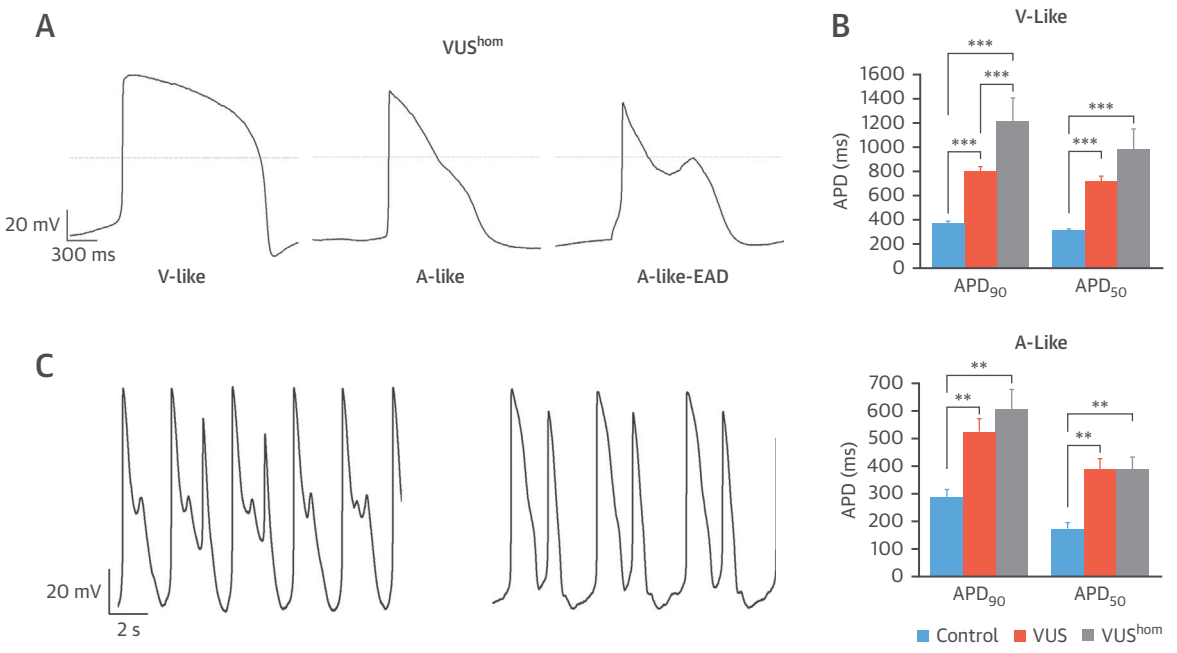

(A) Representative AP recordings from genome-edited homozygous variant of uncertain significance (VUS^{hom}) iPSC-CMs showing V-like, A-like, and A-like-EAD waveforms. Notice the marked APD prolongation in both V-like and A-like iPSC-CMs. **(B)** The APD_{90}, and APD_{50} values in control (**blue**, n = 49), VUS (**orange**, n = 119), and VUS^{hom} (**gray**, n = 29) A-like and V-like iPSC-CMs. **p < 0.01, ***p < 0.001 when compared with healthy control iPSC-CMs. Error bars show SEM. **(C)** Development of spontaneous arrhythmogenicity in VUS^{hom} iPSC-CMs manifested as EADs **(left)** or triggered beat **(right)**. Abbreviations as in Figures 1 and 2.

observed in voltage dependence of I_{Kr} activation parameters ($V_{1/2}$ and k) when compared with healthy control or VUS iPSC-CMs (Figure 7G). We also recorded intracellular calcium concentration ($[Ca^{2+}]_i$) transients (elicited by electrical stimulation at 0.5 Hz) from the VUS^{corr} iPSC-CMs and compared it to the VUS iPSC-CMs. Notably, in comparison to VUS, VUS^{corr} iPSC-CMs displayed normal electrical (non-arrhythmic) activity (Online Figure 8A), lower diastolic $[Ca^{2+}]_i$, and acceleration of cytosolic $[Ca^{2+}]_i$ decay as indicated by a faster rate constant and shorter decay tau ($p < 0.001$) (Online Figures 8B to 8E). Taken together, these findings suggest that genome-edited correction of the $KCNH2^{T983I}$ variant influences the I_{Kr} expression and reverses the abnormal phenotype in VUS iPSC-CMs.

DISCUSSION

In recent years, genetic testing has emerged as a routine clinical tool (25) to perform cascade screening of LQTS patients. Although these tests have significantly improved the rapid identification of disease-causing variants in patients, the results are often inconclusive due to incomplete penetrance and variable expressivity (26). This issue is further compounded by the identification of hundreds of VUS in LQTS-susceptibility genes, which is currently based on combining data from population frequency and in silico modeling, along with published data on cosegregation and functional studies in heterologous expression systems (9,10).

Identification of VUS designation in LQTS is clinically important, as these variants may be used to guide genotype-specific management or facilitate rapid screening of potentially at-risk relatives. Unfortunately, this can put candidate patients, families, and ordering physicians in a frustrating state of clinical limbo (27,28). Under such circumstances, patient-specific electrophysiological characterization of these variants to distinguish pathogenic mutations from benign rare variants is crucial not only for accurate diagnosis, but also for appropriate clinical management. This new approach represents a significant advancement for precision medicine in the management of LQTS disorders.

FIGURE 7 Genome-Edited Corrected iPSC-CMs Showed Rescue of Abnormal Phenotype

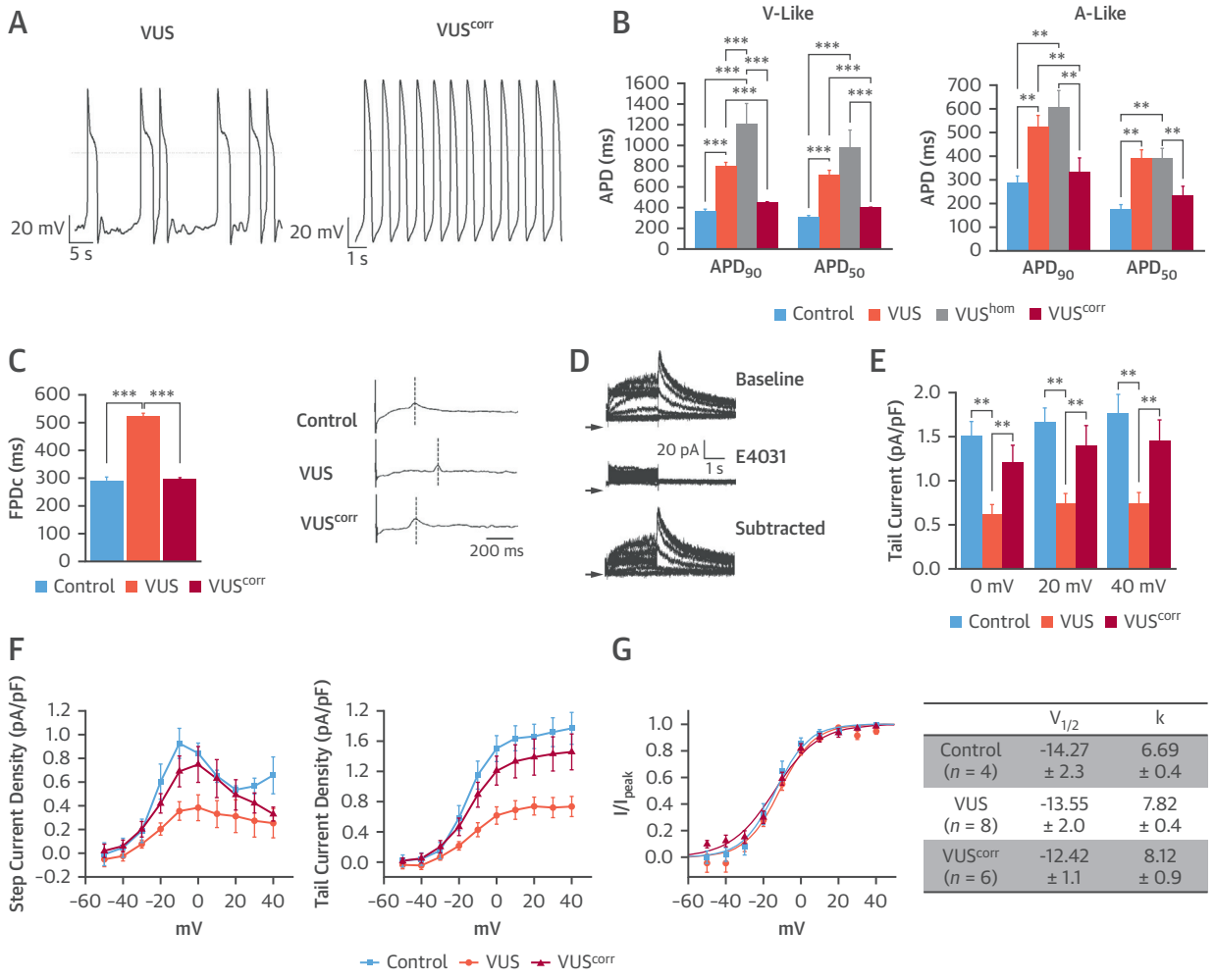

	$V_{1/2}$	k
Control (n = 4)	-14.27 ± 2.3	6.69 ± 0.4
VUS (n = 8)	-13.55 ± 2.0	7.82 ± 0.4
VUS^{corr} (n = 6)	-12.42 ± 1.1	8.12 ± 0.9

(A) Representative AP recordings from **(left)** VUS and **(right)** genome-edited corrected variant of uncertain significance (VUS^{corr}) iPSC-CMs. **(B)** Summary of APD_{90} and APD_{50} from control **(blue)**, VUS **(orange)**, VUS^{hom} **(gray)**, and VUS^{corr} **(red)** iPSC-CMs (**p < 0.01, ***p < 0.001). **(C, left)** Summary of rate-matched FPDc values from control **(blue)**, VUS **(orange)**, and VUS^{corr} **(red)** iPSC-CMs (n = 7). FPDc = FPD/(beat period)$^{0.3333}$. Error bars show SEM. ***p < 0.001. **(C, right)** Representative MEA recordings from control **(top)**, VUS **(middle)**, and VUS^{corr} **(bottom)** iPSC-CM monolayer. **(D)** Single-cell voltage-clamp recordings of I_{Kr}, measured from VUS^{corr} iPSC-CMs. **(Top)** Baseline recordings. **(Middle)** Recording following administration of E-4031 (2 μmol/l). **(Bottom)** E-4031-sensitive current (I_{Kr}) defined by digital subtraction of the 2 currents. **(E)** Summary of peak tail I_{Kr} density in pA/pF from control **(blue)** (n = 4), VUS **(orange)** (n = 8), and VUS^{corr} **(red)** (n = 6) iPSC-CMs at membrane potentials; 0, +20, and +40 mV (**p < 0.01). **(F)** Average I-V curves for I_{Kr} step current **(left)** and tail current **(right)** density in pA/pF for control **(blue)**, VUS **(orange)**, and VUS^{corr} **(red)** iPSC-CMs. **(G, left)** Average peak tail current normalized to the maximal current following repolarization to −40 mV (I/I_{peak}) in control **(blue)**, VUS **(orange)**, and VUS^{corr} **(red)** iPSC-CMs. **(G, right)** Summary of $V_{1/2}$ and k parameters of I_{Kr} compared for control, VUS, and VUS^{corr} iPSC-CMs. Mean values ± SEM are shown. Comparison of iPSC lines was performed with 1-way analysis of variance; p < 0.05 was considered statistically significant. Abbreviations as in Figures 1 and 2.

Recent advances in CRISPR genome editing and iPSC-CM platforms can provide a valuable clinical application to decipher the pathogenicity of VUS and better predict arrhythmia risk, but this approach remains unproven to date. Since the original discovery of iPSC technology in 2007, iPSCs have proven to be a robust model for studying various cardiac disease mechanisms (29-31), for drug screening (17,32,33), and for validating a KCNJ2 variant (10), despite their relative immaturity with respect to human adult cardiomyocytes. Although iPSC-based models for verified LQT2 mutations such as severely

CENTRAL ILLUSTRATION **Patient-in-a-Dish Platform for Elucidating Variant of Uncertain Significance Pathogenicity**

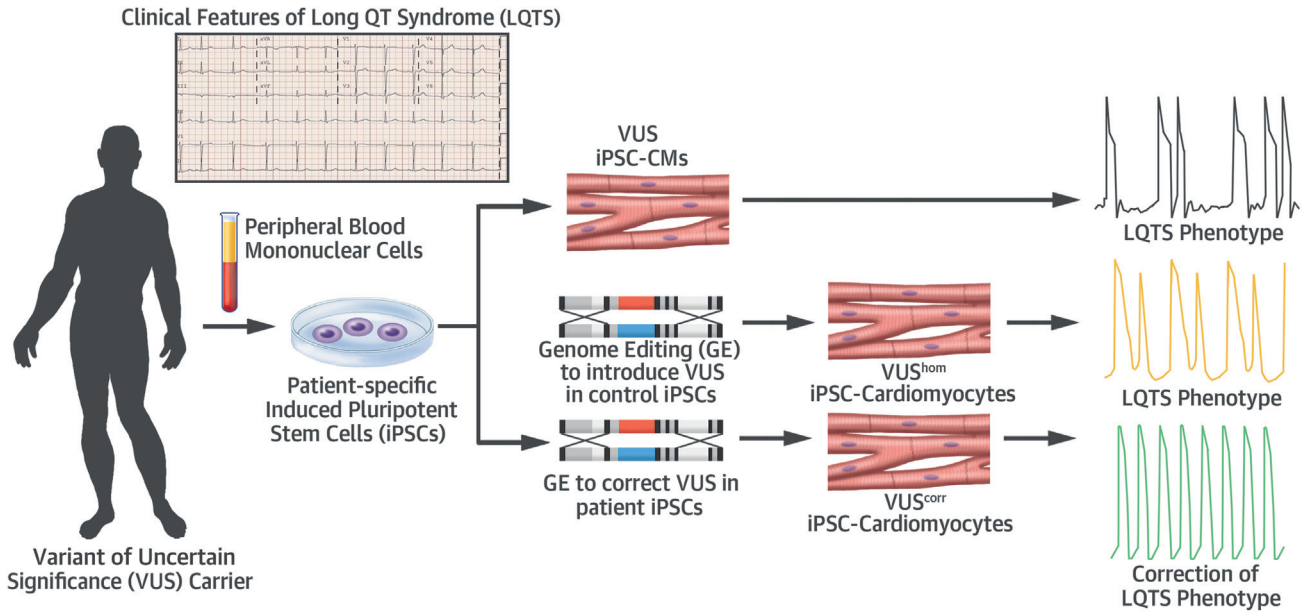

Garg, P. et al. J Am Coll Cardiol. 2018;72(1):62–75.

Patient-specific iPSC-CMs generated from a VUS ($KCNH2^{T983I}$) carrier exhibited prolonged APD due to reduced I_{Kr} density compared with healthy control cells **(black trace).** Introduction of the homozygous variant in the healthy control iPSCs recapitulated a severe LQTS phenotype **(yellow trace)**, whereas correction of the VUS in patient iPSCs rescued the observed electrophysiological abnormalities **(green trace)**. Thus, genome editing of iPSC-CMs can potentially offer a unique precision medicine approach to decipher VUS pathogenicity in a dish. This robust approach may bring a major advancement in the care of LQTS patients to improve their quality of life and appropriately manage their risk of sudden death. APD = action potential duration; GE = genome editing; iPSC = induced pluripotent stem cell; iPSC-CM = induced pluripotent stem cell-derived cardiomyocyte; LQTS = long QT syndrome; VUS = variant of uncertain significance; VUS^{corr}, genome-edited corrected variant of uncertain significance; VUS^{hom}, genome-edited homozygous variant of uncertain significance.

symptomatic A614V (14), A561T (16), and asymptomatic R176W (15) mutations in KCNH2 have been previously reported, VUS that lack any functional data or family history were not studied for LQT2 using the iPSC platform.

In the present study, healthy control and VUS iPSCs were differentiated into functional cardiomyocytes, and detailed electrophysiological analysis was performed. Consistent with the patient's clinical phenotype, VUS iPSC-CMs recapitulated the hallmark features of LQTS disorder, including a delayed repolarization and mild arrhythmogenicity compared with the healthy control cells. Although APD prolongation was observed in 54% of total cells recorded, only 12.9% of cells exhibited arrhythmogenic activity that manifested as EADs. These findings suggest that similar to studies on asymptomatic R176W by Lahti et al. (15) and in contrast to more severe phenotype reported by Itzhaki et al. (14) and Matsa et al. (16), the T983I variant exhibits mild arrhythmogenicity. Moreover, MEA analysis performed on a monolayer of cells revealed a significant prolongation of the FPDc in VUS iPSC-CMs compared with healthy control cells, corroborating the single-cell patch clamp results. Finally, calcium imaging studies also confirmed an increased incidence of arrhythmia and higher diastolic calcium in VUS iPSC-CMs compared to isogenic control iPSC-CMs.

To further investigate the underlying mechanism of the variant pathogenicity, single-cell voltage-clamp recordings of I_{Kr} were performed. We observed a 41% to 44% decrease in I_{Kr} tail current density in VUS versus healthy control iPSC-CMs. The I_{Kr} density values obtained in our control lines (1.46 to 1.77 pA/pF) are in agreement with I_{Kr} previously reported in iPSC-CMs (0.55 to 1.9 pA/pF) (14,15). Importantly, biophysical analysis of hERG WT (control) and hERG T983I (VUS) further revealed that the

mutant channels exhibited largely similar voltage dependence of gating as the WT channels based on the activation parameters. Furthermore, Western blot data confirmed that the underlying mechanism of the variant pathogenicity is reduced total hERG protein and deficiency of mature channel trafficking to the cell surface.

In previous reports, LQTS iPSC-CMs have been shown to exhibit a higher sensitivity to proarrhythmia due to their already compromised repolarization reserve when compared with healthy control cells (15,17). Consistent with the repolarization reserve hypothesis (34), VUS iPSC-CMs displayed enhanced proarrhythmicity to CiPA high-risk torsadogenic drugs such as dofetilide, ibutilide, and azimilide. In contrast, treatment with a recently discovered hERG channel activator (ICA-105574) enhanced I_{Kr} density and normalized APD in VUS iPSC-CMs, suggesting a potential pharmacotherapy for LQT2-specific patients. Collectively, these findings support the notion that I_{Kr} is implicated in the disease mechanism encoded by the $KCNH2^{T983I}$ variant.

A unique advantage of genome editing technology in disease modeling is the ability to study variants in an isogenic background to rule out phenotypic variability from epigenetic differences or unknown genetic modifiers. In addition, in a reciprocal approach, genome editing can be used to correct known variants in iPSC lines to generate isogenic controls for comparison, rather than using unrelated samples or unaffected family members (35). Using the CRISPR/Cas9 genome editing approach, we first introduced the homozygous variant T983I in a healthy control line and then corrected the variant in the patient line followed by examination of the electrophysiological properties of both genome-edited lines. Similar to our findings in the parent lines, the genome-edited homozygous line (VUS^{hom}) exhibited characteristic LQTS phenotype with significantly prolonged APDs and generation of baseline arrhythmias, such as EADs and triggered activity. In line with our hypothesis, and similar to the verified LQT2 mutation A561V, the VUS^{hom} iPSC-CMs had a higher percentage of baseline arrhythmias compared with the heterozygous patient VUS line. In contrast, the corrected line (VUS^{corr}) exhibited properties similar to the healthy control line, confirming the causative role of the underlying single KCNH2 mutation in the patient.

STUDY LIMITATIONS. A major limitation of iPSC-CMs is that they are relatively immature with respect to ion channel and calcium handling properties compared to adult human cardiomyocytes (36). Moreover, this study was focused on a single LQT2 variant for validating the iPSC and genome-editing platform. In the future, other LQTS variants need to be investigated to further validate the sensitivity of the approach.

CONCLUSIONS

We generated iPSC-CMs from a VUS carrier of LQT2 and demonstrated their abnormal electrophysiological phenotype. We delineated VUS pathogenicity by using genome editing to selectively correct the variant in KCNH2 to normalize the aberrant cellular phenotype, and finally introduced the homozygous KCNH2 variant in an otherwise healthy individual to exacerbate the disease phenotype (**Central Illustration**). These findings provide the first report of utilizing iPSC-CMs and CRISPR genome editing technology as tools to examine the pathogenicity of VUS in LQTS. This stands to add to the yield of clinical genetic testing in this population and advance the care of patients with LQTS to improve their quality of life and appropriately manage their risk of SCD. In the future, this approach can be expanded to other channelopathies to accelerate progress toward realizing the promise of precision medicine in inherited arrhythmia.

ACKNOWLEDGMENT The authors thank Kathryn C. Claiborn for critical reading of the manuscript.

ADDRESS FOR CORRESPONDENCE: Dr. Joseph C. Wu, Lorry I. Lokey Stem Cell Research Building, 265 Campus Drive, Room G1120, Stanford, California 94305-5111. E-mail: joewu@stanford.edu. Twitter: @StanfordCVI.

PERSPECTIVES

COMPETENCY IN MEDICAL KNOWLEDGE: Selective genome editing of patient-specific cardiomyocytes derived from iPSCs can identify pathogenic variants in an in vitro model of arrhythmogenic cardiac channelopathy and correct the aberrant cellular phenotype.

TRANSLATIONAL OUTLOOK: Future studies based on human iPSCs and genome editing could provide a personalized approach to drug therapy for patients with congenital LQTS and other inherited conditions associated with cardiac arrhythmias.

REFERENCES

1. Schwartz PJ, Stramba-Badiale M, Crotti L, et al. Prevalence of the congenital long-QT syndrome. Circulation 2009;120:1761–7.

2. Schwartz PJ, Crotti L, Insolia R. Long-QT syndrome: from genetics to management. Circ Arrhythm Electrophysiol 2012;5:868–77.

3. Roden DM. Clinical practice. Long-QT syndrome. N Engl J Med 2008;358:169–76.

4. Anderson ME. "We are not alone": ion channel mutations in a long QT syndrome cohort. Heart Rhythm 2005;2:1106–7.

5. Giudicessi JR, Ackerman MJ. Genetic testing in heritable cardiac arrhythmia syndromes: differentiating pathogenic mutations from background genetic noise. Curr Opin Cardiol 2013;28:63–71.

6. Priori SG, Napolitano C, Schwartz PJ. Low penetrance in the long-QT syndrome: clinical impact. Circulation 1999;99:529–33.

7. Kaufman ES, Priori SG, Napolitano C, et al. Electrocardiographic prediction of abnormal genotype in congenital long QT syndrome: experience in 101 related family members. J Cardiovasc Electrophysiol 2001;12:455–61.

8. Marjamaa A, Salomaa V, Newton-Cheh C, et al. High prevalence of four long QT syndrome founder mutations in the Finnish population. Ann Med 2009;41:234–40.

9. Li B, Mendenhall JL, Kroncke BM, et al. Predicting the functional impact of KCNQ1 variants of unknown significance. Circ Cardiovasc Genet 2017;10:e001754.

10. Gélinas R, El Khoury N, Chaix M-A, et al. Characterization of a human induced pluripotent stem cell-derived cardiomyocyte model for the study of variant pathogenicity: validation of a KCNJ2 mutation. Circ Cardiovasc Genet 2017;10:e001755.

11. Fusaki N, Ban H, Nishiyama A, Saeki K, Hasegawa M. Efficient induction of transgene-free human pluripotent stem cells using a vector based on Sendai virus, an RNA virus that does not integrate into the host genome. Proc Jpn Acad Ser B Phys Biol Sci 2009;85:348–62.

12. Mehta A, Sequiera GL, Ramachandra CJ, et al. Re-trafficking of hERG reverses long QT syndrome 2 phenotype in human iPS-derived cardiomyocytes. Cardiovasc Res 2014;102:497–506.

13. Lian X, Hsiao C, Wilson G, et al. Robust cardiomyocyte differentiation from human pluripotent stem cells via temporal modulation of canonical Wnt signaling. Proc Natl Acad Sci U S A 2012;109:E1848–57.

14. Itzhaki I, Maizels L, Huber I, et al. Modelling the long QT syndrome with induced pluripotent stem cells. Nature 2011;471:225–9.

15. Lahti AL, Kujala VJ, Chapman H, et al. Model for long QT syndrome type 2 using human iPS cells demonstrates arrhythmogenic characteristics in cell culture. Dis Model Mech 2012;5:220–30.

16. Matsa E, Dixon JE, Medway C, et al. Allele-specific RNA interference rescues the long-QT syndrome phenotype in human-induced pluripotency stem cell cardiomyocytes. Eur Heart J 2014;35:1078–87.

17. Liang P, Lan F, Lee AS, et al. Drug screening using a library of human induced pluripotent stem cell-derived cardiomyocytes reveals disease-specific patterns of cardiotoxicity. Circulation 2013;127:1677–91.

18. Wang Y, Liang P, Lan F, et al. Genome editing of isogenic human induced pluripotent stem cells recapitulates long QT phenotype for drug testing. J Am Coll Cardiol 2014;64:451–9.

19. Fatima A, Kaifeng S, Dittmann S, et al. The disease-specific phenotype in cardiomyocytes derived from induced pluripotent stem cells of two long QT syndrome type 3 patients. PLoS One 2013;8:e83005.

20. Sanguinetti MC. HERG1 channel agonists and cardiac arrhythmia. Curr Opin Pharmacol 2014;15:22–7.

21. Zhang H, Zou B, Yu H, et al. Modulation of hERG potassium channel gating normalizes action potential duration prolonged by dysfunctional KCNQ1 potassium channel. Proc Natl Acad Sci U S A 2012;109:11866–71.

22. Gerlach AC, Stoehr SJ, Castle NA. Pharmacological removal of human ether-a-go-go-related gene potassium channel inactivation by 3-nitro-N-(4-phenoxyphenyl) benzamide (ICA-105574). Mol Pharmacol 2010;77:58–68.

23. Asayama M, Kurokawa J, Shirakawa K, et al. Effects of an hERG activator, ICA-105574, on electrophysiological properties of canine hearts. J Pharmacol Sci 2013;121:1–8.

24. Cavero I, Holzgrefe H. Comprehensive in vitro Proarrhythmia Assay, a novel in vitro/in silico paradigm to detect ventricular proarrhythmic liability: a visionary 21st century initiative. Expert Opin Drug Saf 2014;13:745–58.

25. Kapplinger JD, Tester DJ, Salisbury BA, et al. Spectrum and prevalence of mutations from the first 2,500 consecutive unrelated patients referred for the FAMILION long QT syndrome genetic test. Heart Rhythm 2009;6:1297–303.

26. Amin AS, Pinto YM, Wilde AA. Long QT syndrome: beyond the causal mutation. J Physiol 2013;591:4125–39.

27. Ackerman MJ. Genetic purgatory and the cardiac channelopathies: Exposing the variants of uncertain/unknown significance issue. Heart Rhythm 2015;12:2325–31.

28. Giudicessi JR. Machine learning and rare variant adjudication in type 1 long QT syndrome. Circ Cardiovasc Genet 2017;10:e001944.

29. Lan F, Lee AS, Liang P, et al. Abnormal calcium handling properties underlie familial hypertrophic cardiomyopathy pathology in patient-specific induced pluripotent stem cells. Cell Stem Cell 2013;12:101–13.

30. Sun N, Yazawa M, Liu J, et al. Patient-specific induced pluripotent stem cells as a model for familial dilated cardiomyopathy. Sci Transl Med 2012;4:130ra47.

31. Liang P, Sallam K, Wu H, et al. Patient-specific and genome-edited induced pluripotent stem cell-derived cardiomyocytes elucidate single-cell phenotype of Brugada syndrome. J Am Coll Cardiol 2016;68:2086–96.

32. Harris K, Aylott M, Cui Y, Louttit JB, McMahon NC, Sridhar A. Comparison of electrophysiological data from human-induced pluripotent stem cell-derived cardiomyocytes to functional preclinical safety assays. Toxicol Sci 2013;134:412–26.

33. Mehta A, Ramachandra CJA, Singh P, et al. Identification of a targeted and testable antiarrhythmic therapy for long-QT syndrome type 2 using a patient-specific cellular model. Eur Heart J 2018;39:1446–55.

34. Roden DM. Long QT syndrome: reduced repolarization reserve and the genetic link. J Intern Med 2006;259:59–69.

35. Bassett AR. Editing the genome of hiPSC with CRISPR/Cas9: disease models. Mamm Genome 2017;28:348–64.

36. Lundy SD, Zhu WZ, Regnier M, Laflamme MA. Structural and functional maturation of cardiomyocytes derived from human pluripotent stem cells. Stem Cells Dev 2013;22:1991–2002.

KEY WORDS arrhythmia, genome editing, induced pluripotent stem cells, long QT syndrome, variant of uncertain significance

APPENDIX For an expanded Methods section as well as supplemental figures and a table, please see the online version of this paper.